

1N-39  
160256  
P.13

# The Influence of Primary and Secondary Orientations on the Elastic Response of a Nickel-Base Single-Crystal Superalloy

Ali Abdul-Aziz and Sreeramesh Kalluri  
*Sverdrup Technology, Inc.*  
*Lewis Research Center Group*  
*Brook Park, Ohio*

and

Michael A. McGaw  
*National Aeronautics and Space Administration*  
*Lewis Research Center*  
*Cleveland, Ohio*

Prepared for the  
38th ASME International Gas Turbine and Aeroengine Congress and Exposition  
sponsored by the American Society of Mechanical Engineers  
Cincinnati, Ohio, May 24-27, 1993



(NASA-TM-106125) THE INFLUENCE OF  
PRIMARY AND SECONDARY ORIENTATIONS  
ON THE ELASTIC RESPONSE OF A  
NICKEL-BASE SINGLE-CRYSTAL  
SUPERALLOY (NASA) 13 p

N93-26550

Unclass

G3/39 0160256



# THE INFLUENCE OF PRIMARY AND SECONDARY ORIENTATIONS ON THE ELASTIC RESPONSE OF A NICKEL-BASE SINGLE-CRYSTAL SUPERALLOY

**Ali Abdul-Aziz and Sreeramesh Kalluri**

Sverdrup Technology, Inc.,  
NASA Lewis Research Center Group  
Cleveland, Ohio

**Michael A. McGaw**

NASA Lewis Research Center  
Cleveland, Ohio

## ABSTRACT

The influence of primary orientation on the elastic response of a [001]-oriented nickel-base single-crystal superalloy, PWA 1480, was investigated under mechanical, thermal, and combined thermal and mechanical loading conditions using finite element techniques. Elastic stress analyses were performed using the MARC finite element code on a square plate of PWA 1480 material. Primary orientation of the single crystal superalloy was varied in increments of  $2^\circ$ , from  $0^\circ$  to  $10^\circ$ , from the [001] direction. Two secondary orientations ( $0^\circ$  and  $45^\circ$ ) were considered, with respect to the global coordinate system, as the primary orientation angle was varied. The stresses developed within the single crystal plate were determined for each loading condition. In this paper, the influence of the angular offset between the primary crystal orientation and the loading direction on the elastic stress response of the PWA 1480 plate is presented for different loading conditions. The influence of primary orientation angle, when constrained between the bounds considered, was not found to be as significant as the influence of the secondary orientation angle, which is not typically controlled.

## INTRODUCTION

Nickel base superalloys have attracted considerable interest for use in rocket and gas turbine engines due to

the superiority of their material properties at high temperature operating conditions (Chandler, 1985). Initial development of these alloys began in the 1960's for application as turbine blade and vane materials. Pratt and Whitney Aircraft was among the first to manufacture single crystal blades, using PWA 1409 which is the single crystal version of Mar-M200 (Kear and Pearcey, 1967). Since that time many other engine companies have developed similar alloys. However, the alloy of interest in this work is the single crystal superalloy PWA 1480 (SC PWA 1480) developed by Pratt and Whitney. This superalloy, which is a well characterized nickel-base cubic single crystal, was selected by Pratt and Whitney as the blade material for the Alternate Turbopump Development Program for the Space Shuttle Main Engine (SSME).

The turbine blades of SC PWA 1480 are directionally solidified such that the span direction is along the low modulus [001] crystallographic direction to enhance creep and thermal fatigue resistance. There is some variation in the [001] orientation of the single crystal from one blade to another due to the manufacturing process. However, it is generally controlled to be within  $10^\circ$  of span direction for all of the turbine blades. The transverse orientation or the secondary crystal orientation [010] is not controlled, and is randomly oriented with respect to a fixed geometric axis in the turbine blade. However, using a seed crystal during solidification will allow control of the secondary

orientation (Duhl, 1989). The single crystal superalloys exhibit cubic symmetry. Three independent elastic constants are required to describe the elastic behavior of a cubic single crystal (Nye, 1957 and Yang, 1984). Their elastic stress-strain relationships are highly orientation dependent (Bowen, et al., 1986 and Abdul-Aziz, et al., 1989). In a previous study, the influence of the secondary orientation on the elastic response of SC PWA 1480 was documented (Kalluri, et al., 1991).

The objective of this work is to determine the influence of the primary orientation on the elastic response of [001]-oriented, SC PWA 1480 under thermal, mechanical, and combined thermal and mechanical loads by conducting finite element stress analyses. The analyses were conducted by varying the primary orientation [001] in increments of  $2^\circ$  from  $0^\circ$  to  $10^\circ$  with respect to a global coordinate system. Two secondary orientations of  $0^\circ$  and  $45^\circ$  with respect to the global coordinate system were found to represent two extreme conditions in a previous study (Kalluri, et al., 1991), and were selected for investigation in the present study. The stresses developed within the SC PWA 1480 material were determined for each loading condition and the influence of the angular offset between the primary crystal orientation and the global coordinate system is discussed for the two secondary orientations considered.

## PROBLEM DESCRIPTION

The turbine blade of a rocket engine turbopump is schematically represented in Fig. 1. This hollow blade is made of SC PWA 1480 and is directionally cast such that the [001] crystallographic direction (primary orientation) is offset with respect to the Z-axis by an angle no greater than  $10^\circ$ . In this design, the hollow core extends below the platform into the shank region. In Figure 1, XYZ is the global coordinate system, with the Z-axis along the span, Y-axis along the chord and the X-axis along the thickness of the blade.

The turbopump blades in a cryogenic liquid propellant rocket engine are cooled except for their airfoils which are typically exposed to the hot gas flow path that can induce high thermal gradients both along the span and through the thickness. For this hollow core blade, the thermal gradient through the thickness may be of the order of  $875^\circ\text{C/cm}$ , while being much milder along the

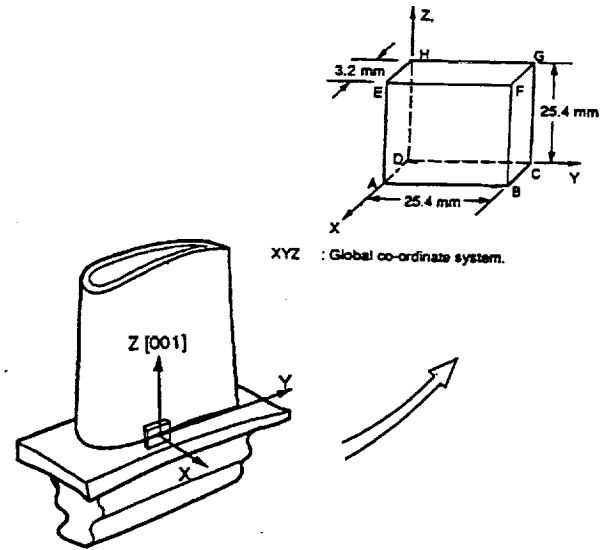
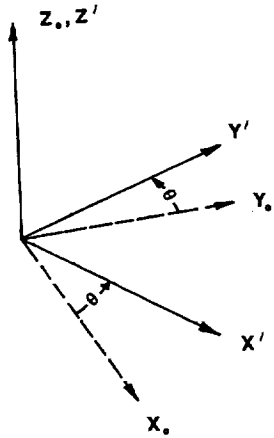


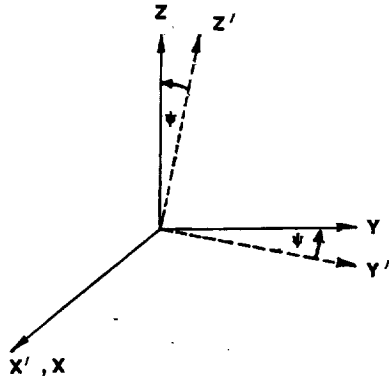
FIG. 1: SCHEMATICS OF SSME TURBINE BLADE AND THE SQUARE PLATE USED IN THE ANALYSIS.

span. These gradients are quite high compared to aircraft turbine engine blades. For example, the first stage high pressure fuel turbopump blade of the SSME is exposed to an extremely high temperature environment where the gas temperature reaches approximately  $2000^\circ\text{C}$  at start-up conditions. Lee et al. (1991) have conducted a 3-D elastic finite element analysis to investigate the stress state of a single crystal hollow core blade with respect to the secondary orientation variations. The temperature bounds used in the current analysis are in agreement with the temperature range used in the investigation by Lee, et al. (1991).

The turbopump blade has complex geometry which makes the thermal and mechanical stress analyses under these severe operating conditions very complicated. Therefore, to investigate the effects of both the primary and secondary orientations under thermal and mechanical operating conditions, an analysis of a square plate made of SC PWA 1480, which is subjected to similar loading conditions will be employed (Fig. 1). A plate with the dimensions of 25.4 mm by 25.4 mm by 3.2 mm was selected for the parametric finite element stress analyses.



(a) ROTATION ABOUT THE Z-AXIS



(b) ROTATION ABOUT THE X'-AXIS

FIG. 2: CRYSTAL AND GLOBAL COORDINATE SYSTEMS

The choice of the plate dimensions was based on convenience and simplicity, except for the thickness which represented the wall thickness of the hollow core blade's airfoil-shank region. The crystal ( $X_c Y_c Z_c$ ) and global ( $XYZ$ ) coordinate systems for the plate are shown in Fig. 2. The crystal coordinate system  $X_c Y_c Z_c$  is first rotated about the  $Z_c$ -axis by an angle  $\theta$  to obtain the  $X' Y' Z'$  coordinate system. The  $X' Y' Z'$  coordinate system is then rotated about the  $X'$ -axis by an angle  $\psi$  to obtain the global coordinate system,  $XYZ$ . The rotation angles  $\psi$  and  $\theta$  among the coordinate

systems represent the orientations of the primary and secondary crystallographic directions, respectively. The matrices of direction cosines that relate the global coordinate system ( $XYZ$ ) to the crystal coordinate system ( $X_c Y_c Z_c$ ) (Fig. 2) are given in the following relationships:

a) Rotating about the  $Z_c$ -axis

$$\begin{pmatrix} x' \\ y' \\ z' \end{pmatrix} = \begin{bmatrix} \cos\theta & \sin\theta & 0 \\ -\sin\theta & \cos\theta & 0 \\ 0 & 0 & 1 \end{bmatrix} \begin{pmatrix} x_c \\ y_c \\ z_c \end{pmatrix} \quad (1)$$

b) Rotating about the  $X'$ -axis

$$\begin{pmatrix} x \\ y \\ z \end{pmatrix} = \begin{bmatrix} 1 & 0 & 0 \\ 0 & \cos\psi & \sin\psi \\ 0 & -\sin\psi & \cos\psi \end{bmatrix} \begin{pmatrix} x' \\ y' \\ z' \end{pmatrix} \quad (2)$$

The transformation matrix is simply obtained by multiplying the above two matrices, Equations (1) and (2). The result of this multiplication is represented in the following:

$$\begin{pmatrix} x \\ y \\ z \end{pmatrix} = \begin{bmatrix} \beta_{11} & \beta_{12} & \beta_{13} \\ \beta_{21} & \beta_{22} & \beta_{23} \\ \beta_{31} & \beta_{32} & \beta_{33} \end{bmatrix} \begin{pmatrix} x_c \\ y_c \\ z_c \end{pmatrix} \quad (3)$$

With,

$$\begin{aligned} \beta_{11} &= \cos\theta \\ \beta_{12} &= \sin\theta \\ \beta_{13} &= 0 \\ \beta_{21} &= -\cos\psi\sin\theta \\ \beta_{22} &= \cos\psi\cos\theta \\ \beta_{23} &= \sin\psi \\ \beta_{31} &= \sin\psi\sin\theta \\ \beta_{32} &= -\sin\psi\cos\theta \\ \beta_{33} &= \cos\psi \end{aligned}$$

Equation (3) is the direction cosine matrix and  $\beta_{ij}$  ( $i,j=1,3$ ) are the corresponding direction cosines.

## ANALYTICAL PROCEDURE

### A. Elastic Stiffness Coefficients

To describe the elastic behavior of a cubic single crystal such as the SC PWA 1480 within the crystallographic coordinate system, three independent elastic stiffness coefficients ( $C_{11}$ ,  $C_{12}$  and  $C_{44}$ ) are required (Nye, 1957). This stiffness matrix for a cubic single crystal in the crystal coordinate system is given in Equation (4).

$$C = \begin{bmatrix} C_{11} & C_{12} & C_{12} & 0 & 0 & 0 \\ C_{12} & C_{11} & C_{12} & 0 & 0 & 0 \\ C_{12} & C_{12} & C_{11} & 0 & 0 & 0 \\ 0 & 0 & 0 & C_{44} & 0 & 0 \\ 0 & 0 & 0 & 0 & C_{44} & 0 \\ 0 & 0 & 0 & 0 & 0 & C_{44} \end{bmatrix} \quad (4)$$

The elastic behavior in the global coordinate system can be described by transformation of the stiffness tensor from the crystal coordinate system to the global coordinate system (Fig. 2) according to the law of transformation of fourth rank tensors. Lieberman and Zirinsky (1956) developed a method for transforming the stiffness coefficients of a single crystal between two coordinate systems that are related by a matrix of direction cosines, Equation (3). Their method was applied to derive the elastic stiffness coefficients of a cubic single crystal in the global coordinate system. The stiffness matrix of the cubic single crystal within the global coordinate system  $[C']$  is given by the following relationship, (Eq. (5)):

$$[C'] = [\beta][C][\beta]^T \quad (5)$$

where  $[C']$  is a 6×6 stiffness matrix in the global coordinate system. The stiffness coefficients for a given set of the primary and secondary orientation angles form a 6×6 matrix that is defined in terms of the directional cosines (Eq. (3)) and is documented by Lieberman and Zirinsky (1956). Thus, Equations (4) and (5) define the stiffness matrix for a cubic single crystal in a global coordinate system (XYZ) that is offset by two angles, the secondary orientation angle  $\theta$  and the primary orientation angle  $\psi$ , to the crystal coordinate system ( $X_c Y_c Z_c$ ; Fig. 2). The relationships among the stresses and strains in the global coordinate system with the transformed stiffness matrix are given by:

$$[\sigma] = [C'][\epsilon] \quad (6)$$

where,

$$\{\sigma\}^T = \{\sigma_{xx} \sigma_{yy} \sigma_{zz} \tau_{yz} \tau_{zx} \tau_{xy}\} \quad (7)$$

and,

$$\{\epsilon\}^T = \{\epsilon_{xx} \epsilon_{yy} \epsilon_{zz} \gamma_{yz} \gamma_{zx} \gamma_{xy}\} \quad (8)$$

In Equation (7),  $\sigma_{xx}$ ,  $\sigma_{yy}$ ,  $\sigma_{zz}$  and  $\tau_{yz}$ ,  $\tau_{zx}$ ,  $\tau_{xy}$  are the engineering normal and shear stresses, and in Equation (8),  $\epsilon_{xx}$ ,  $\epsilon_{yy}$ ,  $\epsilon_{zz}$  and  $\gamma_{yz}$ ,  $\gamma_{zx}$ ,  $\gamma_{xy}$  are the engineering normal and shear strains, respectively. The three independent elastic stiffness coefficients for the SC PWA 1480 material at various temperatures were obtained from Kalluri et al. (1991).

The secondary orientation angles, of 0° and 45°, were selected for investigation because a previous study with the same exact boundary conditions conducted on SC PWA 1480 (Kalluri et al., 1991) showed that the stiffness coefficients have a periodicity of 90°, with the secondary orientation angle,  $\theta$ . It was also found in that study that the stresses generated were maximum at  $\theta=45^\circ$  and minimum at  $\theta=0^\circ$ , which made these two secondary orientations to be the logical choices for future investigations. However, for the primary orientation angle,  $\psi$ , the range chosen was from 0° to 10° because manufacturing tolerance is typically 10° for  $\psi$ .

## B. FINITE ELEMENT ANALYSIS

The elastic stress analyses were carried out using the MARC Finite Element code. These calculations were initiated by setting up a physical representation of the problem through the construction of a finite element model for the square plate geometry. The model consisted of 500 isoparametric eight-noded solid elements with 1040 nodes and was generated using PATRAN (1989). Ten elements were generated along the sides and five elements were used through the thickness of the plate, (Fig. 3).

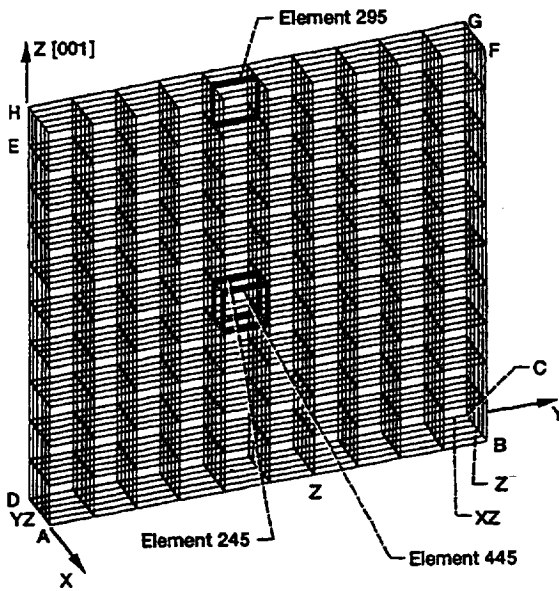


FIG. 3: FINITE ELEMENT MESH OF THE SQUARE PLATE.

The stress analyses were conducted by running a heat transfer analysis followed by a subsequent elastic stress analysis. In order to ensure equilibrium and avoid rigid body motion, the following mechanical boundary conditions were imposed (Fig. 3): (1) the node at D was fixed in the X, Y, & Z directions, (2) nodes along the edge AD were fixed in the Y & Z directions, (3) nodes along the edge DC were fixed in the X & Z directions and (4) nodes along edges AB and BC were fixed in the Z direction. Enforcement of all these boundary conditions was implemented by invoking the Fixed Boundary option in the finite element program. Five

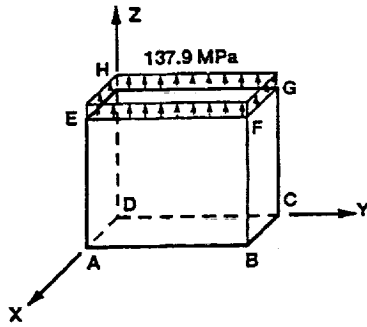
different loading cases were considered in this work: mechanical, thermal (two cases), and combined mechanical and thermal (two cases). The previously listed boundary conditions were employed in all five loading cases.

**1. Heat Transfer Analysis.** Thermal loads with gradients along both X and Z directions were applied to the model, Figures 4(b) and 4(c). Choice of imposing the thermal gradients along these two directions was an attempt to simulate gradients through the thickness and along the span of a turbine blade. The other loading case involved a distributed mechanical load of 137.9 MPa along the Z-direction, Figure 4(a). Other loading conditions investigated were combined mechanical and thermal loads for the two directions considered (X and Z).

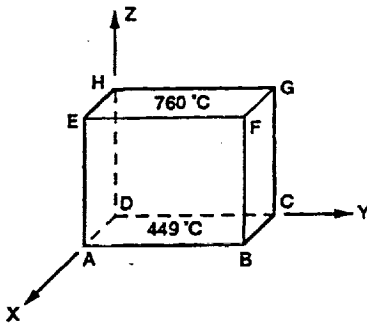
The single crystal PWA 1480 is a thermally isotropic material. All physical properties used for the analyses including the mean coefficient of thermal expansion, thermal conductivity, and specific heat were documented by Kalluri et al. (1991). The thermal boundary conditions imposed were representative of those typically experienced by rocket engine turbine blades. Figure 4 shows the thermal gradients employed, which closely represent the SSME turbine blade temperatures at full power level conditions. Plate surfaces, noted on Figure 4(b) and (c) with the designated temperatures assigned to them, were added to the thermal model in MARC Finite Element code and the rest of the faces were assumed to be insulated. Output from the thermal analysis was used as an input for the subsequent elastic stress analyses.

**2. Stress Analysis.** The stiffness coefficient matrices for the various primary orientations ( $\psi=0^\circ$  to  $10^\circ$  in increments of  $2^\circ$ ) and for the selected secondary orientations ( $\theta=0^\circ$  and  $45^\circ$ ) were all incorporated in the finite element calculations through the MARC Finite Element code. In addition, the temperature dependencies of all the physical properties were used.

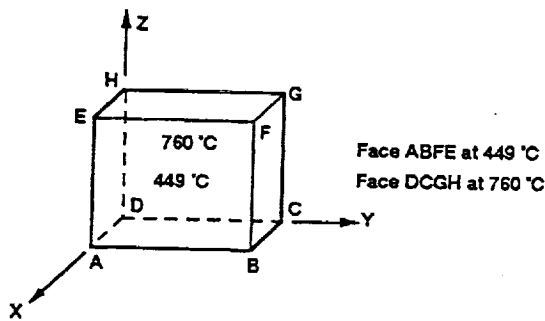
To maintain consistency and to compare with the study conducted previously on secondary orientation effects (Kalluri et al., 1991), the elements shown in Fig. 3 were selected to document the variations in the stress



(a) DISTRIBUTED MECHANICAL LOAD  
ALONG Z-AXIS



(b) THERMAL GRADIENT ALONG Z-AXIS



(c) THERMAL GRADIENT ALONG X-AXIS

FIG. 4: LOADING CASES IMPOSED ON  
THE SQUARE PLATE.

components as the primary and secondary orientations were varied. The reason behind the choice of these elements, as described by Kalluri et al. (1991), was mainly to capture the locations that represent the true effects of the loading imposed, and not the effects of thermal and mechanical constraints applied. These elements are: Element 295, located near surface EFGH for the thermal load in the Z-direction case, where a thermal gradient is imposed through faces ABCD and EFGH, element 445 for the thermal load in the X-direction case (thermal gradient through faces DCGH and ABFE) and element 295 for the mechanical loading case.

### DISCUSSION OF ANALYTICAL RESULTS

In this study, the influence of both primary and secondary orientation angles on the elastic response of SC PWA 1480 was determined under different thermal and mechanical loading conditions. For each element and loading case, the individual stress components at given primary and secondary orientation angles  $\psi$  and  $\theta$  were normalized with the corresponding stress components obtained for  $\psi=0^\circ$ ,  $\theta=0^\circ$  or  $45^\circ$ , i.e.  $(\sigma_{xx})_{\psi,\theta}/(\sigma_{xx})_{0,0}$ ,  $(\sigma_{yy})_{\psi,\theta}/(\sigma_{yy})_{0,0}$ ,  $(\tau_{xy})_{\psi,\theta}/(\tau_{xy})_{0,0}$ , and so on. For each secondary orientation angle considered, the individual as well as the normalized components were plotted against the primary orientation angle  $\psi$ , for each element and loading condition. Figures 5 to 10 show these plots as a function of the primary orientation angle  $\psi$ , for fixed secondary orientation angles of  $\theta=0^\circ$  and  $45^\circ$ .

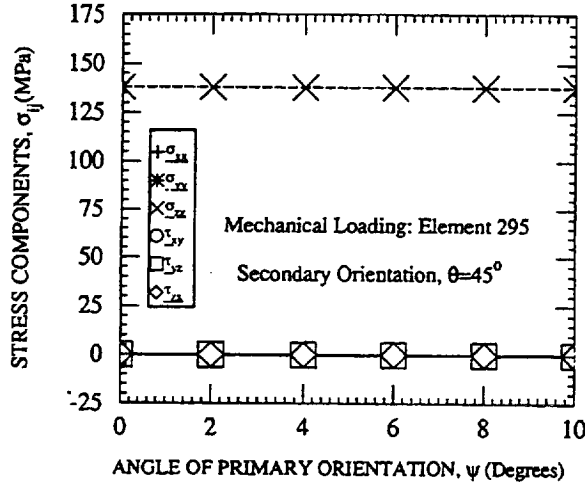
Figure 5<sup>1</sup> shows the influence of the primary orientation on the elastic response for element 295 for a secondary orientation angle of  $\theta=45^\circ$  under mechanical loading only. The variations of the individual and normalized stress components with the primary orientation angle are shown in Figs. 5(a) and 5(b) respectively. None of the stress components shown in Fig. 5(a) varied significantly as  $\psi$  changed from  $0^\circ$  to  $10^\circ$ . The normalized components, Fig. 5(b), exhibited some variation with  $\psi$ , however, these variations are not substantial, because the magnitudes of the respective

<sup>1</sup> The graphics software used to draw these figures superimposes the data symbols with the last symbol on top. The rest of the data symbols, as shown in the key for each figure, are underneath this symbol.

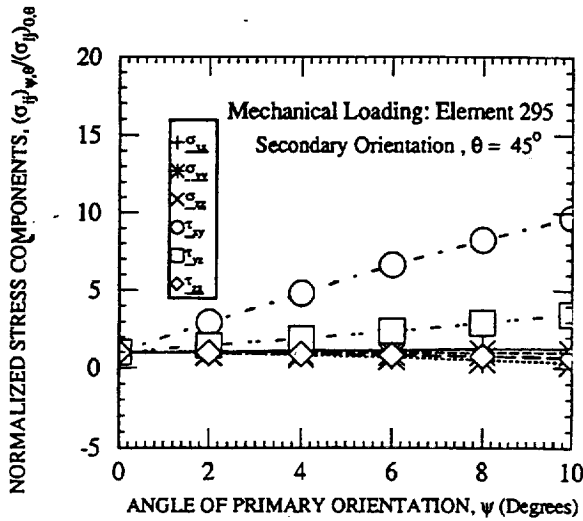


individual stress components are rather small. Thus, it should be realized that the variations in the normalized stress components with  $\psi$ , while indicative of the influence of the primary orientation on the elastic response of the SC PWA 1480, alone are not sufficient to assess the importance of the primary orientation effects. The variations in the actual magnitudes of the

individual components of stress also must be considered to determine the quantitative significance of the orientation effects. The stresses generated in elements 245 and 445 under mechanical loading for  $\theta=45^\circ$  were similar to those presented in Fig. 5. In addition, for element 295, similar results were observed for  $\theta=0^\circ$ , under mechanical loading.

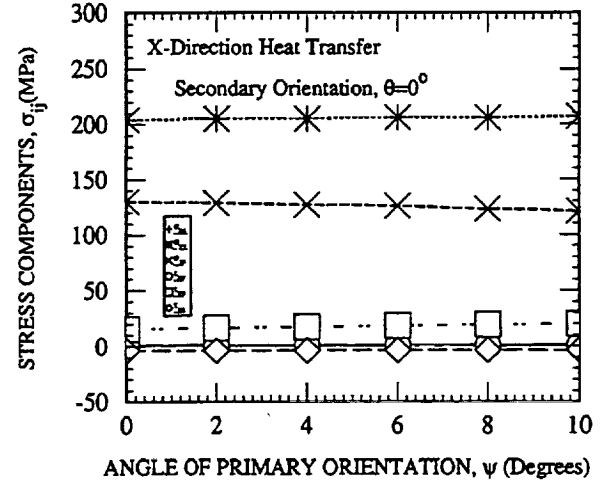


(a) INDIVIDUAL STRESS COMPONENTS.

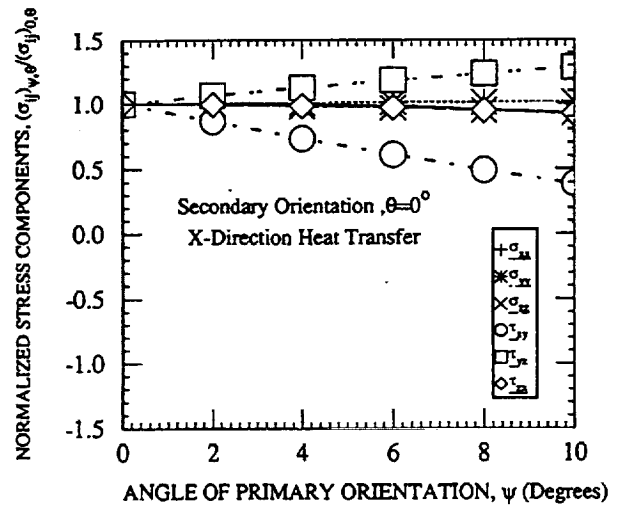


(b) NORMALIZED STRESS COMPONENTS

FIG. 5: INFLUENCE OF PRIMARY ORIENTATION ANGLE ON STRESS COMPONENTS UNDER IMPOSED MECHANICAL LOADING FOR ELEMENT 295.

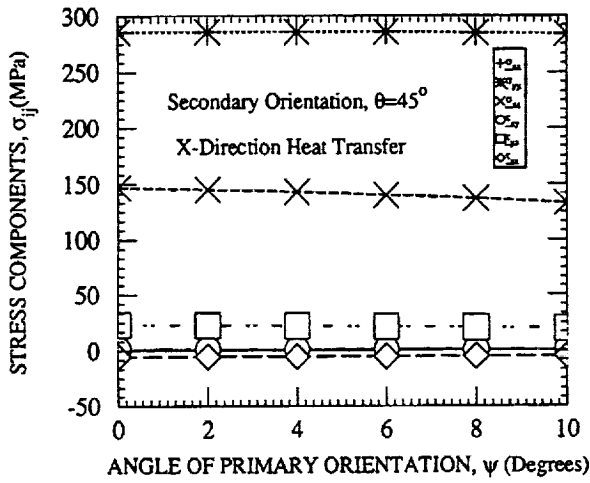


(a) INDIVIDUAL STRESS COMPONENTS

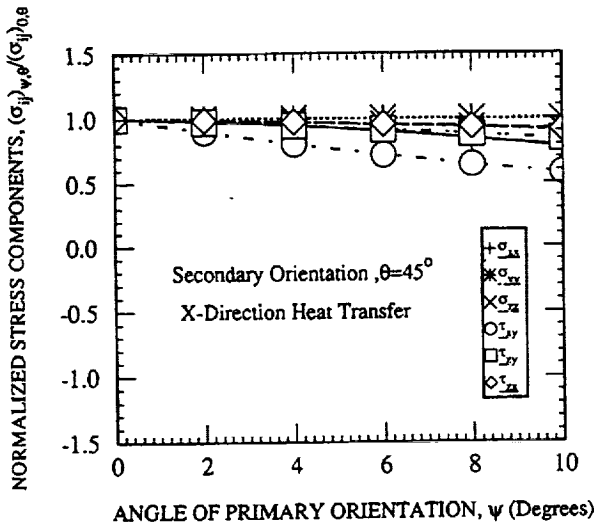


(b) NORMALIZED STRESS COMPONENTS

FIG. 6: VARIATION OF STRESS COMPONENTS WITH PRIMARY ORIENTATION ANGLE UNDER THERMAL LOADS FOR ELEMENT 445 ( $\theta=0^\circ$ ).

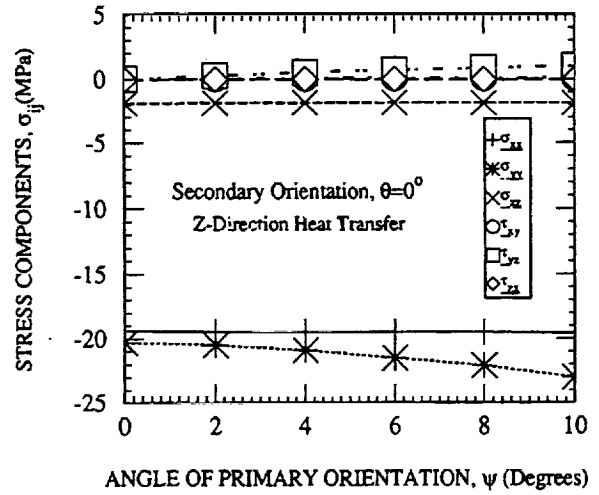


(a) INDIVIDUAL STRESS COMPONENTS

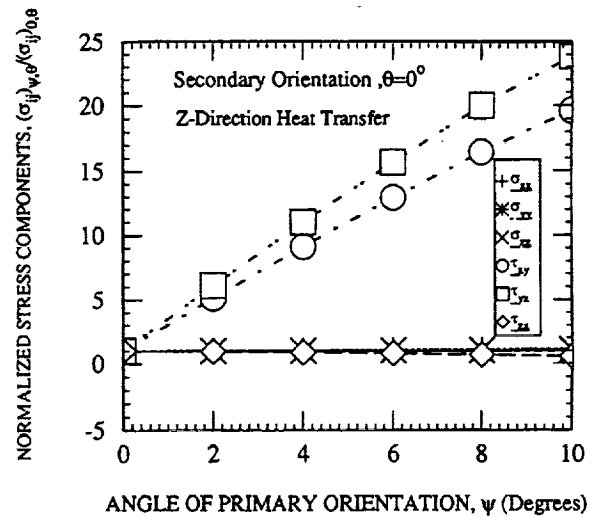


(b) NORMALIZED STRESS COMPONENTS

FIG. 7: VARIATION OF STRESS COMPONENTS WITH PRIMARY ORIENTATION ANGLE UNDER THERMAL LOADS FOR ELEMENT 445 ( $\theta=45^\circ$ ).



(a) INDIVIDUAL STRESS COMPONENTS



(b) NORMALIZED STRESS COMPONENTS

FIG. 8: VARIATION OF STRESS COMPONENTS WITH PRIMARY ORIENTATION ANGLE UNDER THERMAL LOADS FOR ELEMENT 295 ( $\theta=0^\circ$ ).

Figures 6(a)-(b) and 7(a)-(b) present the variations of the individual and normalized stress components with

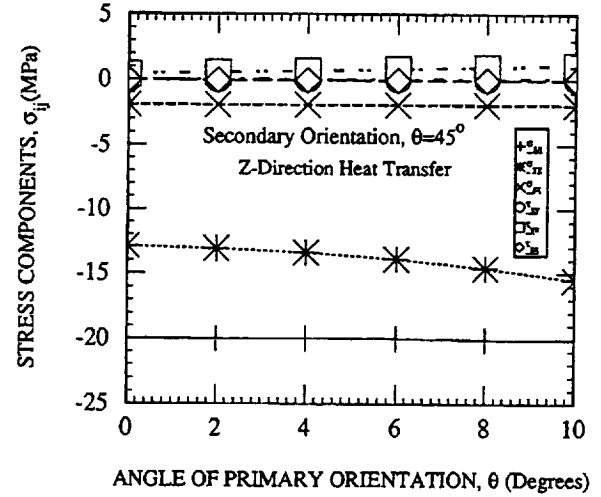
the primary orientation angle for secondary orientations of  $0^\circ$  and  $45^\circ$  under thermal loads along the X-

direction for element 445. The stress components in Figs. 6(a) and 7(a) show small variations with  $\psi$  except for  $\sigma_{yy}$  and  $\sigma_{zz}$ , which exhibited noticeable variations with  $\psi$ . The magnitudes of the  $\sigma_{yy}$  and  $\sigma_{zz}$  components for  $\theta=45^\circ$  are 16 percent and 41 percent larger, respectively, than the corresponding magnitudes for  $\theta=0^\circ$ . This clearly indicates that a secondary orientation angle of  $45^\circ$  is undesirable for any primary orientation angle,  $\psi$ , between  $0^\circ$  and  $10^\circ$ . The normalized stress components, Figures 6(b) and 7(b), show slight variations as  $\psi$  increases for both secondary orientations considered ( $\theta=0^\circ$  and  $\theta=45^\circ$ ).

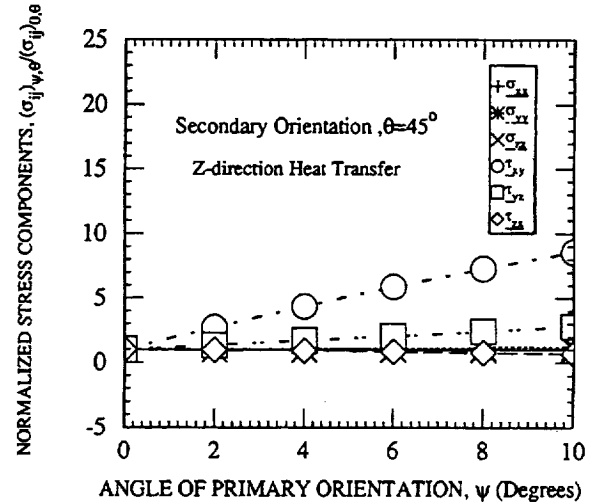
Figures 8(a) and 9(a) show the stress components under thermal loading along Z-axis for element 295. The  $\sigma_{yy}$  component is lower for  $\theta=45^\circ$  than for  $\theta=0^\circ$ , and both change as  $\psi$  changes from  $0^\circ$  to  $10^\circ$ . The normalized stress components, Figs. 8(b) and 9(b),  $(\tau_{xy})_{\psi,\theta}/(\tau_{xy})_{0,\theta}$  and  $(\tau_{yz})_{\psi,\theta}/(\tau_{yz})_{0,\theta}$ , have exhibited large variations with  $\psi$ . However, these variations, which are due to orientation changes as well as loading conditions, are not significant because of the relatively small magnitudes of these stress components.

The stress components for element 295 under combined thermal and mechanical loading conditions were observed to obey the principle of superposition of linear elastic loadings. For this case, the normalized stress components for  $\theta=0^\circ$  and  $\theta=45^\circ$  exhibited similar variation with  $\psi$  as those observed in the case of pure thermal loading along the Z-axis, Figs. 8 (b) and 9 (b). For brevity, figures of the individual and normalized stress components for the combined loading conditions for element 295 are not included.

Figure 10 shows the stress components in element 445 for combined thermal and mechanical loading with thermal loading applied along the X-axis as the primary orientation changes from  $\psi=0^\circ$  to  $\psi=10^\circ$ , for  $\theta=0^\circ$  and  $\theta=45^\circ$ . The changes in the stress components with  $\psi$  are small, which leads to the conclusion that the primary orientation does not have a significant effect on the elastic response under these conditions. However, the magnitudes of  $\sigma_{yy}$  and  $\sigma_{zz}$ , for a given  $\psi$ , were 41 and 29 percent larger, respectively, for  $\theta=45^\circ$  than the corresponding magnitudes for  $\theta=0^\circ$ . As mentioned earlier for the loading case involving X-directional thermal load, the secondary orientation of  $\theta=45^\circ$  generated large stresses and hence should be avoided for thermal loads involving X-directional gradients.



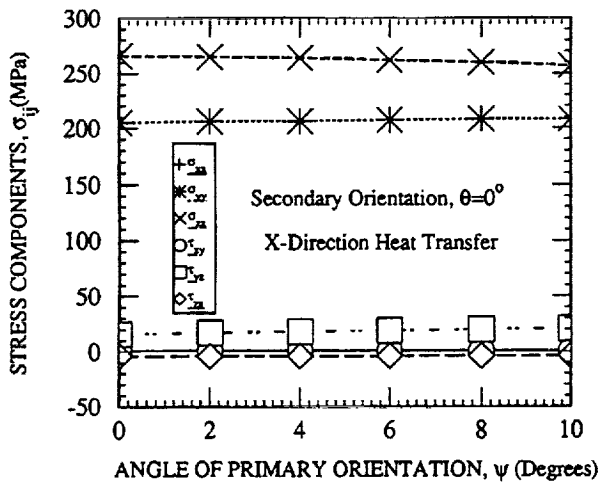
(a) INDIVIDUAL STRESS COMPONENTS



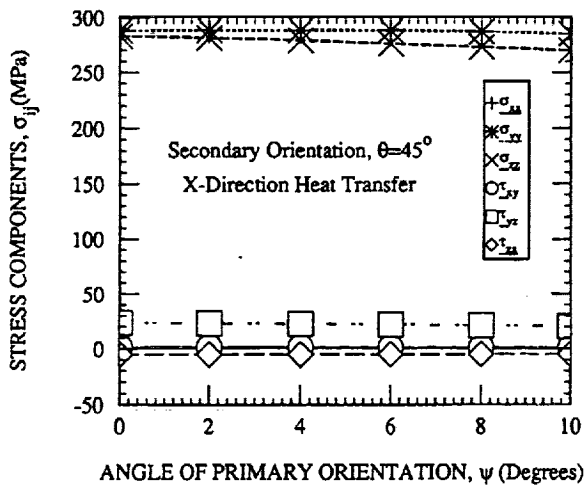
(b) NORMALIZED STRESS COMPONENTS

FIG. 9: VARIATION OF STRESS COMPONENTS WITH PRIMARY ORIENTATION ANGLE UNDER THERMAL LOADS FOR ELEMENT 295 ( $\theta=45^\circ$ ).

The normalized components for the combined thermal (along the X-direction) and mechanical loading case varied in a similar manner with  $\psi$  as in the case of pure thermal loading along the X-direction, Figs. 6(b) and 7(b). It was found that the thermal gradient through the thickness had produced much larger stresses than that along the length (primary orientation of [001]) of the plate. This is because the thermal gradient through the thickness of the plate is much larger than that along Z-



(a) INDIVIDUAL STRESS COMPONENTS  
AT  $\theta=0^\circ$



(b) INDIVIDUAL STRESS COMPONENTS  
AT  $\theta=45^\circ$

FIG. 10: VARIATION OF STRESS COMPONENTS  
WITH PRIMARY ORIENTATION ANGLE UNDER  
THERMAL AND MECHANICAL LOADS FOR  
ELEMENT 445.

axis. In addition, Lee. et al. (1991) analyzed a single crystal blade and the temperature bounds that they used corresponded with the data adopted to run this study, specifically, thermal gradients and magnitudes of

temperatures.

## CONCLUDING REMARKS

A parametric study was conducted using elastic finite element stress analysis to determine the influence of primary orientation angle, at two different secondary orientation angles of  $0^\circ$  and  $45^\circ$ , on the elastic behavior of [001]-oriented nickel base single crystal superalloy, PWA 1480 under mechanical, thermal, and combined thermal and mechanical loads. The primary orientation angle was varied from  $0^\circ$  to  $10^\circ$  in increments of  $2^\circ$  and the stresses developed within a single crystal PWA 1480 square plate under different loading conditions were computed. The following conclusions were drawn from this study:

(1) The type of loading (mechanical, thermal, or combined) imposed on the square plate dictated the variation in the individual stress components with the primary and the secondary orientation angles. Variation of primary and secondary orientation angles did not influence the stresses generated within the single crystal PWA 1480 plate under the purely mechanical loading condition. However, under thermal and combined thermal and mechanical loading conditions, influence of both primary and secondary orientations was observed.

(2) Accurate evaluation of the primary and secondary orientation effects should include consideration of the magnitudes of the individual stress components in addition to the normalized stress components for each loading condition.

(3) The influence of the primary orientation angle, when constrained between  $0^\circ$  and  $10^\circ$ , on the elastic stresses generated within the single crystal PWA 1480 is substantially lower than the influence of secondary orientation angle, which is not typically controlled.

## REFERENCES

- Abdul-Aziz, A., August, R. and Nagpal, V., 1989, "Design Considerations for a Space Shuttle Main Engine (SSME) Turbine Blade Made of Single Crystal Material", AIAA/AHS/ASME Aircraft Design, Systems and Operations Conference, AIAA-89-2149.
- Bowen, K., Nagy, P., and Parr, R. A., 1986, "The Evaluation of Single Crystal Superalloys for Turbopump Blades in the SSME", AIAA/ASME/SAE/ASME 22nd

Joint Propulsion Conference, AIAA-86-1477.

Chandler, W. T., 1985, "Materials for Advanced Rocket Engine Turbopump Turbine Blades", Advanced High Pressure O<sub>2</sub>/H<sub>2</sub> Technology, NASA CP 2372, pp. 110-132.

Duhl, D. N., 1989, "Single Crystal Superalloys", Superalloys, Supercomposites and Superceramics, J. K. Tien and T. Caulfield, Eds., Academic Press, Inc., pp. 149-155.

Kear, B.H., and Pearcey, B.J., 1967, "Tensile and Creep Properties of Single Crystals of the Nickel-Base Superalloy Mar-M200", Trans. AIME, Vol. 239, 1209.

Kalluri, S., Abdul-Aziz, A. and McGaw, M. A. , 1991, "Elastic Response of [001]-Oriented PWA 1480 Single Crystal-- The Influence of Secondary Orientation", SAE Technical Paper series, No. 911111, Presented at the 1991 Aerospace Atlantic Meeting in Dayton, Ohio.

Lee, H. M., and Franck C. G., 1991, "Analysis of a Single Crystal Turbine Blade for the Space Shuttle main Engines", Proceedings ANSYS. 5th International Conference and Exhibition, Volume 2, Session 12, pg. 67, Pittsburgh, Pa.

Lieberman, D.S., and Zirinsky, S., 1956, "A Simplified Calculation for the Elastic Constants of Arbitrarily Oriented Single Crystals", Acta Cryst., 9, pp. 431-436.

MARC General Purpose Finite Element Analysis Program, 1988, Vol. A: User Information Manual; Vol. B: Marc Element Library; Vol. F: Theoretical Manual. MARC Analysis Corporation, Palo Alto, CA.

Nye, J. F., 1957, "Physical Properties of Crystals, Their Representation by Tensors and Matrices", Clarendon Press, Oxford, pp. 131-149.

PATRAN Plus Graphic and Finite elements Package, 1989, Volume I and II, PDA Engineering, Costa Mesa, California.

Yang, S., 1984, " Elastic Constants of a Monocrystalline Nickel-Base Superalloy", Metallurgical Transactions, Vol. 16 A, p. 661.

REPORT DOCUMENTATION PAGE			Form Approved OMB No. 0704-0188	
Public reporting burden for this collection of information is estimated to average 1 hour per response, including the time for reviewing instructions, searching existing data sources, gathering and maintaining the data needed, and completing and reviewing the collection of information. Send comments regarding this burden estimate or any other aspect of this collection of information, including suggestions for reducing this burden, to Washington Headquarters Services, Directorate for Information Operations and Reports, 1215 Jefferson Davis Highway, Suite 1204, Arlington, VA 22202-4302, and to the Office of Management and Budget, Paperwork Reduction Project (0704-0188), Washington, DC 20503.				
1. AGENCY USE ONLY (Leave blank)	2. REPORT DATE April 1993	3. REPORT TYPE AND DATES COVERED Technical Memorandum		
4. TITLE AND SUBTITLE The Influence of Primary and Secondary Orientations on the Elastic Response of a Nickel-Base Single-Crystal Superalloy		5. FUNDING NUMBERS  WU-553-13-00		
6. AUTHOR(S)  Ali Abdul-Aziz, Sreeramesh Kalluri, and Michael A. McGaw				
7. PERFORMING ORGANIZATION NAME(S) AND ADDRESS(ES)  National Aeronautics and Space Administration Lewis Research Center Cleveland, Ohio 44135-3191		8. PERFORMING ORGANIZATION REPORT NUMBER  E-7801		
9. SPONSORING/MONITORING AGENCY NAME(S) AND ADDRESS(ES)  National Aeronautics and Space Administration Washington, D.C. 20546-0001		10. SPONSORING/MONITORING AGENCY REPORT NUMBER  NASA TM-106125		
11. SUPPLEMENTARY NOTES Prepared for the 38th ASME International Gas Turbine and Aeroengine Congress and Exposition sponsored by the American Society of Mechanical Engineers, Cincinnati, Ohio, May 24-27, 1993. Ali Abdul-Aziz and Sreeramesh Kalluri, Sverdrup Technology, Inc., Lewis Research Center Group, 2001 Aerospace Parkway, Brook Park, Ohio 44142. Michael A. McGaw, NASA Lewis Research Center. Responsible person, Michael A. McGaw, (216) 433-3308.				
12a. DISTRIBUTION/AVAILABILITY STATEMENT  Unclassified - Unlimited Subject Category 39			12b. DISTRIBUTION CODE	
13. ABSTRACT (Maximum 200 words)  The influence of primary orientation on the elastic response of a [001]-oriented nickel-base single-crystal superalloy, PWA 1480, was investigated under mechanical, thermal, and combined thermal and mechanical loading conditions using finite element techniques. Elastic stress analyses were performed using the MARC finite element code on a square plate of PWA 1480 material. Primary orientation of the single crystal superalloy was varied in increments of 2°, from 0° to 10°, from the [001] direction. Two secondary orientations (0° and 45°) were considered, with respect to the global coordinate system, as the primary orientation angle was varied. The stresses developed within the single crystal plate were determined for each loading condition. In this paper, the influence of the angular offset between the primary crystal orientation and the loading direction on the elastic stress response of the PWA 1480 plate is presented for different loading conditions. The influence of primary orientation angle, when constrained between the bounds considered, was not found to be as significant as the influence of the secondary orientation angle, which is not typically controlled.				
14. SUBJECT TERMS  Stress analysis; Single-crystal superalloy; Primary orientation; Secondary orientation			15. NUMBER OF PAGES 12	
			16. PRICE CODE A03	
17. SECURITY CLASSIFICATION OF REPORT Unclassified	18. SECURITY CLASSIFICATION OF THIS PAGE Unclassified	19. SECURITY CLASSIFICATION OF ABSTRACT Unclassified	20. LIMITATION OF ABSTRACT	